Influence of environmental stability on the regulation of end-point impedance during the maintenance of arm posture

Matthew A. Krutky, Randy D. Trumbower and Eric J. Perreault

J Neurophysiol 109:1045-1054, 2013. First published 5 December 2012;
doi: 10.1152/jn.00135.2012

J Neurophysiol 109: 1045–1054, 2013.
First published December 5, 2012; doi:10.1152/jn.00135.2012.

Influence of environmental stability on the regulation of end-point impedance during the maintenance of arm posture

Matthew A. Krutky,[1,3] Randy D. Trumbower,[1,4] and Eric J. Perreault[1,2,3]

[1]*Sensory Motor Performance Program, Rehabilitation Institute of Chicago, Chicago, Illinois;* [2]*Department of Physical Medicine and Rehabilitation, Northwestern University, Chicago, Illinois;* [3]*Department of Biomedical Engineering, Northwestern University, Evanston, Illinois; and* [4]*Department of Rehabilitation Medicine, Emory University, Atlanta, Georgia*

Submitted 13 February 2012; accepted in final form 29 November 2102

Krutky MA, Trumbower RD, Perreault EJ. Influence of environmental stability on the regulation of end-point impedance during the maintenance of arm posture. *J Neurophysiol* 109: 1045–1054, 2013. First published December 5, 2012; doi:10.1152/jn.00135.2012.—Many common tasks compromise arm stability along specific directions. Such tasks can be completed only if the impedance of the arm is sufficient to compensate for the destabilizing effects of the task. During movement, it has been demonstrated that the direction of maximal arm stiffness, the static component of impedance, can be preferentially increased to compensate for directionally unstable environments. In contrast, numerous studies have shown that such control is not possible during postural tasks. It remains unknown if these findings represent a fundamental difference in the control of arm mechanics during posture and movement or an involuntary response to the destabilizing environments used in the movement studies but not yet tested during posture maintenance. Our goal was to quantify how arm impedance is adapted during postural tasks that compromise stability along specific directions. Our results demonstrate that impedance can be modulated to compensate for these instabilities during postural tasks but that the changes are modest relative to those previously reported during reaching. Our observed changes were primarily in the magnitude of end-point stiffness, but these were not sufficient to alter the direction of maximal stiffness. Furthermore, there were no substantial changes in the magnitude of end-point viscosity or inertia, suggesting that the primary change to arm impedance was a selective increase in stiffness to compensate for the destabilizing stiffness properties of the environment. We suggest that these modest changes provide an initial involuntary response to destabilizing environments prior to the larger changes that can be affected through voluntary interventions.

end-point stiffness; impedance; posture; stretch reflex

COMMON TASKS, SUCH AS THE use of hand tools or writing utensils, compromise the stability of the arm along specific directions (Rancourt and Hogan 2001). These tasks can be completed only if the impedance of the arm is sufficient to compensate for the destabilizing effects of the task. Many postural tasks can be described in terms of their contributions to the coupled stiffness of the arm and the environment (McIntyre et al. 1996). As a result, many postural studies have focused on the end-point stiffness characteristics of the human arm, which define the static component of arm impedance, as measured at the point of contact with the environment. At a fixed posture, changes in muscle activation can be used to regulate end-point stiffness. However, whereas changes in muscle activation can greatly alter the magnitude of end-point stiffness (Mussa-Ivaldi et al. 1985), they have been shown to have only a modest influence on the orientation of maximal stiffness (Darainy et al. 2004; Gomi and Osu 1998; Perreault et al. 2002; Selen et al. 2009). These postural results are in contrast to the dramatic changes in stiffness orientation that have been reported during movement (Burdet et al. 2001; Franklin et al. 2004, 2007). These contrasting results may reflect fundamental differences in the control of posture and movement (Darainy et al. 2007) or may be an effect of the destabilizing environments used in the reaching experiments but not yet evaluated during postural tasks.

Interacting with compliant or unstable loads has been shown to increase the sensitivity of stretch reflexes (Akazawa et al. 1983; Dietz et al. 1994; Doemges and Rack 1992a, b), which can contribute substantially to limb stiffness (Kearney et al. 1997; Sinkjaer 1988; Zhang and Rymer 1997). Recently, we demonstrated (Krutky et al. 2010) that stretch-reflex sensitivity throughout the arm adapts to the directional properties of an unstable environment. When the destabilizing stiffness of the environment exceeds the intrinsic stiffness of the arm, stretch-reflex sensitivity increases specifically to compensate for perturbations along the orientation of the unstable environment. Those results suggest that the involuntary mechanisms associated with stretch-reflex modulation may contribute to a preferential change in end-point stiffness orientation, similar to that reported previously for movements in unstable environments. Quantifying the changes in end-point stiffness during postural interactions with directionally unstable loads is necessary to determine if environmental stabilities alone are sufficient to alter the orientation of maximal stiffness.

The purpose of this study was to quantify changes in three-dimensional (3D) end-point impedance of the human arm during postural interactions with different unstable haptic environments and one stable control environment. The mechanical properties of the unstable environments had the characteristics of a negative-stiffness spring, which has previously been shown to alter reflex sensitivity during postural tasks (Krutky et al. 2010) and also end-point stiffness during movement tasks (Burdet et al. 2001; Franklin et al. 2007). The unstable environments were oriented either along the direction of maximal arm stiffness or orthogonal to that direction. Two stiffness magnitudes were used: one with a magnitude less than the stiffness of the arm measured in a preliminary experiment and one with a magnitude greater than that stiffness. We hypothesized that interactions with directionally unstable environments would cause task-appropriate changes in end-point stiffness. This is the first study to investigate this question during the maintenance of posture using haptic environments directly comparable with those previously shown to drive changes

Address for reprint requests and other correspondence: E. J. Perreault, Depts. of Biomedical Engineering and Physical Medicine and Rehabilitation, Northwestern Univ., 345 E. Superior St., Rm. 1403, Chicago, IL (e-mail: e-perreault@northwestern.edu).

in arm stiffness during movement. The nature of the adaptation observed during these postural tasks provides insight into how arm mechanics are tuned to the mechanical properties of the environment and how that tuning differs during posture and movement control. Preliminary results from this work have been reported previously in extended abstract form (Krutky et al. 2009).

METHODS

Subjects

Eight right-handed subjects, 26 to 29 years of age (six males and two females), participated in this study. No subject had a history of neurological impairment or orthopedic limitations of the upper limbs. Subjects gave written, informed consent and were free to withdraw at any time. This protocol was approved by the Institutional Review Board at Northwestern University (IRB STU00009204). Each subject participated in one preliminary experiment and one primary experiment, performed on separate days. During the preliminary session, we used stochastic perturbations of arm posture to compute a baseline estimate of end-point impedance. During the primary sessions, we investigated how interactions with different haptic environments influenced end-point impedance.

Equipment

Details of the equipment have been provided previously (Trumbower et al. 2009). During all experiments, subjects interacted with a three-degrees-of-freedom (DOF) robotic manipulator (HapticMaster; Moog, The Netherlands; Fig. 1*A*). The robot uses an admittance control algorithm, allowing it to simulate a range of haptic environments (Van der Linde et al. 2002). During the preliminary experiment, the robot was programmed as a stiff (50 kN/m) position servo, and stochastic perturbations were used to estimate arm impedance. During the primary experiments, the robot was programmed to simulate an unstable haptic environment; while subjects interacted with this environment, the robot was transiently switched to a stiff position servo so that a rapid perturbation could be applied for the estimation of limb impedance. The switch from an unstable to stiff haptic environment occurred in <1 ms (Krutky et al. 2010). The robot was instrumented to measure end-point displacements and forces, both recorded at 1.25 kHz.

Subjects were attached rigidly to the robot using a custom-fitted cast. The cast extended approximately one-third of the distance from the wrist to the elbow, fixing the wrist in a neutral position. The cast was mounted to a low-mass custom gimbal attached to the end of the manipulator, allowing the application of pure end-point forces and no moments to the arm. The gimbal was instrumented with potentiometers that were used to provide subjects with visual feedback of arm posture so that a fixed posture could be maintained throughout each trial. The gimbal's center was positioned along the axis of the forearm, under the third metacarpophalangeal joint, which we defined as the end point of the limb for these experiments. Subjects were seated during these experiments and harnessed at the shoulders and waist to an immobile chair.

As subjects interacted with the robot, end-point displacement was measured redundantly with an optical motion analysis system (Optotrak 3020; Northern Digital, Waterloo, Ontario, Canada), with a resolution of 0.1 mm. The optical tracking data were used to correct for small differences between the displacement of the subject's hand and the displacement estimated using the robot sensors. This difference arises from the compliance in the transmission between the robot sensors and its end-effector attached to the subject. Although small, this difference would lead to biased estimates of impedance. Unbiased estimated are obtained by the use of optical measurements, not affected by the transmission compliance (Trumbower et al. 2009). The optical tracking system measured the motion of infrared light-emitting diodes, which were mounted on a rigid body attached to a wrist cast and used to monitor end-point location. All optical data were collected at 250 Hz. This measurement system has been validated using mechanical loads with a calibrated stiffness and shown to provide stiffness estimates that are accurate to within 10% when using either the ramp-and-hold or stochastic perturbations described below [Krutky (2009); see Chapter 5].

Protocols

All experiments were performed on the right arm, maintained at a fixed posture. This posture corresponded to the shoulder in ~70° of abduction and ~45° of horizontal flexion. The elbow was flexed at ~90°, and the forearm was in a neutral-to-pronated position, placing the hand directly in front of the glenohumeral joint.

Preliminary experiment: baseline estimate of end-point impedance. Details of the preliminary experiment were identical to those presented previously (Krutky et al. 2010; Trumbower et al. 2009). The purpose of this experiment was to produce an initial estimate of end-point impedance for each subject during interaction with a stiff environment. For this purpose, the robot was programmed as a critically damped, isotropically rigid (50 kN/m) position servo and used to apply stochastic displacements to the end point of the arm.

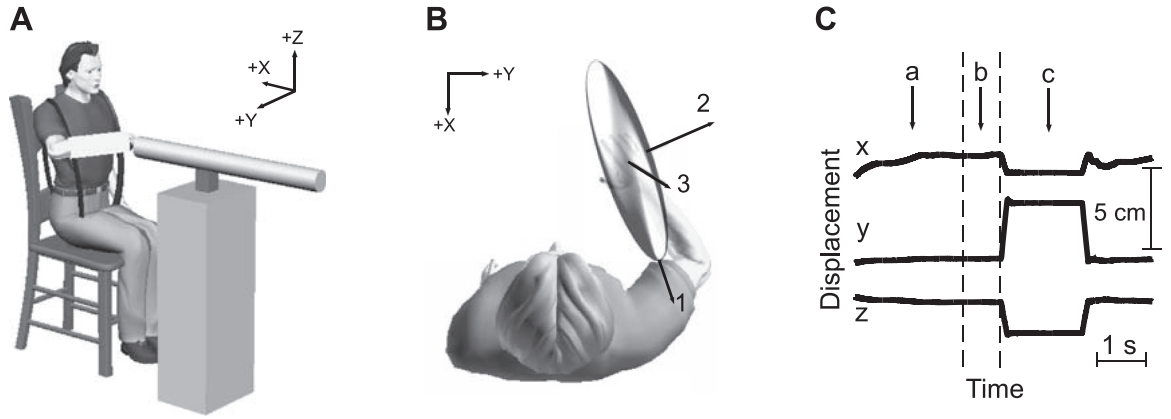

Fig. 1. Experimental setup. *A*: 3-dimensional robotic manipulator and coordinate system used in all experiments. *B*: orientation of typical end-point stiffness ellipsoid and its associated primary, secondary, and tertiary axes. *C*: typical end-point displacement recorded during a single trial of the primary experiment used to quantify the influence of different destabilizing environments on end-point impedance. *a*: target position and force; *b*: holding this position and force for a uniformly distributed, random period of time between 0.5 s and 1.5 s; *c*: after this time period, a single ramp-and-hold perturbation was applied to the arm. Further details about the end-point displacement characteristics are provided in the text.

Stochastic perturbations were chosen for their high information content and short experimental time. These had a SD of 3 mm and a frequency content that was flat below 5 Hz, beyond which, it decayed at a rate of 40 dB/decade. The subject's task was to maintain a fixed arm posture while maintaining the target force and not to react to the perturbation. Target forces were 10 N in the ±X, ±Y, or ±Z direction (Fig. 1*A*); four separate trials were conducted for each of the six target-force directions. It should be noted that the muscle activation required to reach these force targets was in addition to that required to support the arm against gravity. Real-time visual feedback of end-point force and posture was provided using a computer display.

Primary experiment: adaptation of end-point impedance to different haptic environments. The objective of the primary experiment was to quantify end-point impedance as subjects interacted with four different haptic environments: one that was rigid and three that were unstable. The order of the four environments was randomized across subjects.

The rigid environment was identical to that used in the preliminary experiment. The destabilizing environments were identical to those used previously for assessing stretch-reflex modulation (Krutky et al. 2010). These simulated a negative-stiffness spring, acting along a 3D line. As subjects moved the position of their hand away from the neutral position, the robot pushed the hand further with a force proportional to the distance between the hand and the neutral point; the proportionality constant was the magnitude of the simulated negative stiffness. All movements were constrained to the direction of the haptic instability by virtual walls with a simulated stiffness of 50 kN/m. These haptic instabilities were oriented relative to the end-point stiffness of the arm, the static component of the impedance measured for each subject in the preliminary experiment (Fig. 1*B*). The destabilizing environments were either aligned to the direction of maximal end-point stiffness or aligned in an orthogonal direction along the secondary axis. Two magnitudes of unstable environmental stiffness (K_{ENV}) were evaluated (Table 1). Both were adjusted for each subject based on the results of the preliminary experiments and on the subject's ability to keep the hand within the specified target location. The lower magnitude of K_{ENV}, used for both unstable directions, was selected to be between the magnitude of the arm stiffness measured along the primary and secondary axes. For each subject, we selected the maximum value within this range (increments of 50 N/m) for which the subject could complete the postural task. In all cases, this was limited by the ability to stay within the end-point target while interacting with the orthogonal environment. A higher-strength environment was also evaluated in the direction aligned to maximal end-point stiffness. Again, the specific value was adjusted for each subject to ensure that the task was as challenging as possible but achievable. In all but two subjects, this high-strength environment was greater in magnitude than the maximum stiffness of the arm, measured in the preliminary experiments.

Table 1. *Strength of the negative-stiffness haptic environments used for each subject and the stiffness magnitude along the primary and secondary axes of stiffness as measured for each subject in the preliminary experiment*

	Haptic Stiffness		End-Point Stiffness (N/m)	
Subject	Low Strength	High Strength	Primary Axis	Secondary Axis
1	−500	−1,650	1,462	227
2	−600	−1,800	622	165
4	−600	−1,850	1,994	455
5	−500	−1,550	1,138	314
6	−250	−850	938	217
7	−500	−1,600	751	198
10	−400	−1,300	742	181
11	−700	−2,100	1,711	326

To estimate end-point impedance during interactions with these unstable environments, we used individual ramp-and-hold perturbations rather than the more efficient stochastic perturbations used in the preliminary experiment. Ramp-and-hold perturbations were selected because they are known to elicit substantial stretch reflexes. In contrast, stochastic perturbations often suppress reflex behavior (Kearney et al. 1997). The "ramp" portion of each perturbation had a velocity of 400 mm/s and duration of 100 ms, resulting in a displacement of 4 cm; the "hold" portion was ~1 s. These characteristics were selected to elicit distinct short- and long-latency reflex responses (Lewis et al. 2005) and to match our previous experiment, demonstrating substantial reflex modulation during interactions with unstable environments (Krutky et al. 2010). To apply repeatable perturbations during interactions with the haptic environments, the manipulator was programmed to become rigid, ~1 ms prior to the application of the perturbation, and to return to the previous haptic state immediately after the perturbation was complete (Perreault et al. 2008). This allowed the use of open-loop rather than closed-loop estimation techniques (Ljung 1999; Westwick and Perreault 2011) and permitted us to match our experimental conditions with those used previously (Krutky et al. 2010). Note that only the initial ramp-and-hold portion of the perturbation was used for impedance estimates.

As in the preliminary experiments, the subject's task was to maintain a constant end-point force and fixed arm posture, while not reacting to the applied perturbations. This ensured that during interactions with each of the four environments, posture, end-point position, and end-point force were matched. The target end-point force was 10 N to the right, along the secondary axis of end-point stiffness. This magnitude was chosen to be well below a level likely to result in fatigue (Rohmert 1960). Also, the application of end-point forces should provide input to the motoneuron pool and facilitate the elicitation of consistent involuntary responses to perturbations (Matthews 1986).

Each trial involved having the subject achieve the target position and force (Fig. 1*C*) and hold this position and force for a uniformly distributed, random period of time between 0.5 s and 1.5 s (Fig. 1*C*). After this period of time, a single ramp-and-hold perturbation was applied to the arm (Fig. 1*C*). The direction of the applied perturbations has been described previously (Krutky et al. 2010). In summary, perturbations were applied along the direction of the three principal axes of end-point stiffness for each subject (Fig. 1*B*) so that the recorded displacements and end-point forces spanned three DOF. Approximately 10 perturbations were repeated for each perturbation direction for a total of ~60 perturbations for each environment. The presentation order of perturbation directions was randomized.

It is important to note that the magnitude estimates of end-point stiffness (the static component of impedance) obtained using small, stochastic perturbations are expected to differ substantially from that obtained using ramp-and-hold perturbations. Small, rapid perturbations keep the muscle within the region, whereas short-range stiffness dominates the perturbation response at the muscle and joint levels (Hu et al. 2011; Rack and Westbury 1974). In contrast, estimates of muscle stiffness decrease dramatically when using ramp-and-hold perturbations (Kirsch et al. 1994). For both stochastic and ramp-and-hold perturbations, stiffness estimates decrease with perturbation amplitude (Kirsch et al. 1994; Pfeifer et al. 2012; Shadmehr et al. 1993). We have previously quantified the expected differences in end-point stiffness estimates obtained using stochastic and ramp-and-hold perturbations similar to those used in this study and found that estimates of stiffness magnitude obtained using the stochastic perturbations can be approximately four times greater than those obtained using the larger amplitude ramp-and-hold perturbations [Krutky (2009); see Chapter 5]. For these reasons, it is not possible to directly compare the stiffness magnitudes obtained in the preliminary experiment (Table 1) with the results from the primary experiment reported below. In

contrast to the stiffness magnitudes, stiffness orientation was found to be invariant with respect to perturbation type, justifying the use of the efficient stochastic perturbations in the preliminary experiment.

Analyses

Preliminary estimates of end-point impedance using stochastic perturbations. Preliminary estimates of end-point impedance were made using stochastic displacement perturbations and nonparametric system identification techniques, as described previously (Krutky et al. 2010; Perreault et al. 1999; Trumbower et al. 2009) In summary, nonparametric transfer functions were used to characterize impedance using the end-point force measurements from the manipulator and the displacement measurements from the optical tracking system. These nonparametric responses were parameterized by a system with inertial (I_{ARM}), viscous (B_{ARM}), and elastic (K_{ARM}) properties, each represented by a 3×3 matrix. Parameter fits were restricted to frequencies in the range 0–10 Hz. The goal of the preliminary experiment was to obtain an average estimate of end-point stiffness, the elastic component of impedance, within the range of experimentally tested forces to customize the haptic environments in the primary experiment for each subject. The end-point stiffness (K_{ARM}) was averaged across all target-force directions and repetitions to provide a single estimate for each subject. Stiffness orientation was computed using techniques described by Gomi and Osu (1998). All subsequent destabilizing environments were oriented relative to the primary and secondary axes of the average K_{ARM} estimated for each subject.

For these preliminary estimates of end-point impedance, the quality of both the nonparametric and parametric fits was evaluated for each trial using the multiple correlation coefficient R^2 between the predicted and measured end-point forces. For the nonparametric and parametric fits, the average R^2 value for each over the frequency range of 0–10 Hz was 0.92 ± 0.01 (mean $\pm$ SD) and 0.82 ± 0.04, respectively, and was similar to those reported before (Trumbower et al. 2009).

Adaptation of end-point impedance to different haptic environments. Linear regression was used to estimate end-point impedance from the ramp-and-hold data collected in the primary experiments. First, the preperturbation mean, corresponding to the first 30 ms before any force or displacement response, was computed for each trial and subtracted. Force and displacement data were filtered at 15 Hz using a two-sided, fourth-order, low-pass Butterworth filter to remove the high-frequency noise. The data were numerically differentiated once to calculate velocity and a second time to calculate acceleration. Finally, data were segmented from 50 ms before perturbation onset to 210 ms following perturbation onset; this range was found to provide robust parameter estimates while limiting the amount of data that could be influenced by voluntary intervention (Krutky et al. 2010). Linear regression was then used to estimate the orientation and magnitude of the inertial, viscous, and elastic components of end-point impedance from the measured end-point kinematics and forces. Separate estimates were used to produce 3D ellipsoids for each subject and each environment. The multiple R^2 was used to evaluate the adequacy of these parametric descriptions of end-point impedance.

Environment-driven changes in 3D parameter ellipsoids (K_{ARM}, B_{ARM}, I_{ARM}) were characterized further by adapting analyses that have previously been applied to 2D stiffness ellipses. The shape (Franklin et al. 2007; Gomi and Osu 1998; Perreault et al. 2001) and symmetric/antisymmetric components (Mussa-Ivaldi et al. 1985) of the estimated stiffness ellipsoids were obtained for each subject and environment. Shape was quantified within the plane where the greatest amount of adaptation was observed by dividing the magnitude of the secondary principal axis by that of the primary axis. The symmetric and antisymmetric components were each quantified by the matrix norm and reported as the percentage ratio of the antisymmetric component to the symmetric component. Previous studies have quantified the magnitudes of the symmetric and antisymmetric components of 2D stiffness using the determinant, but this was not possible since the antisymmetric component of a 3×3 matrix is skew symmetric and has a zero determinant.

We used a general linear model to evaluate the hypotheses that interactions with directionally destabilizing environments would cause task-appropriate changes in the end-point stiffness, viscosity, and inertia ellipsoids. Separate analyses were conducted for the magnitude and orientations along each of the primary axes and for the shape and antisymmetric/symmetric components of stiffness. All orientations were measured as rotations relative to the average orientation for each parameter ellipsoid, averaged across all subjects and conditions. The tested environments (rigid, aligned, orthogonal, and high-strength aligned) were considered as a fixed factor, and subjects were treated as a random factor in all linear models. F-tests were used to evaluate the significance of each factor. When the influence of the environmental factor was significant, all pair-wise contrasts were evaluated and corrected for multiple comparisons. Significance was assessed at $P < 0.05$. All statistical calculations were completed with the R for Mac OS X software package, version 2.7.0 (R Development Core Team, Vienna, Austria).

RESULTS

End-Point Kinematics During Postural Maintenance

The haptic environment with which subjects interacted influenced end-point kinematics during the maintenance of posture. The postural kinematics were assessed by computing the end-point tracking error, defined as the average distance between the actual and target end-point positions for 100 ms prior to the perturbation. The environment with which the subject was interacting had a significant effect on tracking error ($F_{3,369} = 18.16$; $P \sim 0$). The tracking errors in the destabilizing environment orthogonal to the direction of maximal arm stiffness (4.2 mm) and the high-strength environment aligned to the direction of maximal stiffness (3.7 mm) were significantly greater than those in the other two environments ($P < 0.05$) but not significantly different from each other. The tracking errors in the rigid (2.1 mm) and low strength-aligned environments (2.8 mm) also were not significantly different from each other.

The magnitude of the tracking errors did not vary with time ($F_{1,369} = 0.01$; $P = 0.93$). This was assessed by comparing the tracking errors for trials corresponding to the first two perturbations in each direction at the beginning of each experiment with the same set of trials at the end of each experiment. This suggests that the subjects' behavior was consistent throughout the duration of these experiments.

Characterization of End-Point Impedance

The haptic environment with which subjects interacted also influenced end-point impedance. These effects could be seen in the force responses to the applied end-point displacements (Fig. 2). For the example shown, the force in the +X direction was increased substantially during interactions with the high-strength environment aligned to maximal stiffness, relative to that recorded during interactions with the isotropically rigid environment. In contrast, there were only moderate changes in the Y and Z components of the end-point force, demonstrating a change in impedance that was largest along a single axis of measurement.

The parametric models of end-point impedance provided an accurate characterization of the measured end-point forces. Across all subjects and environments, the average R^2 between the parametric model predictions and the measured forces was

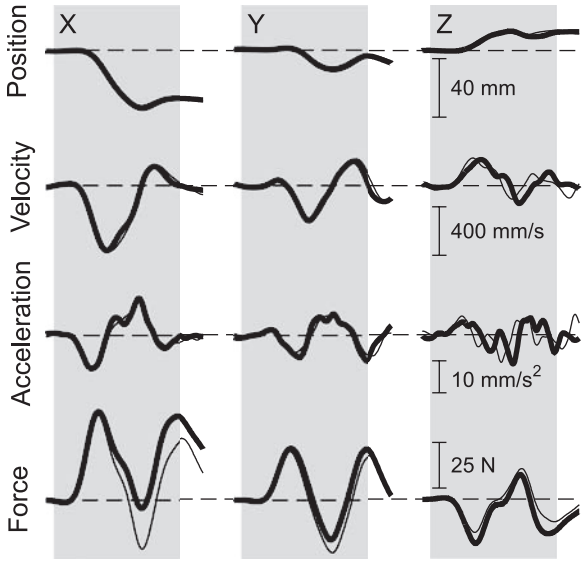

Fig. 2. End-point position, velocity, acceleration, and force data recorded during individual trials with 2 different haptic environments. Thick traces correspond to interactions with the high-strength environment aligned to maximal end-point stiffness; thin traces correspond to interactions with the isotropically rigid environment. For both environments, the subject was applying 10 N along the secondary axis of end-point stiffness, which corresponded to ~2 N in the −X direction, ~9 N in the +Y direction, and ~2 N in the −Z direction. These steady-state values were removed prior to estimating impedance. The shaded blocks correspond to the time window used for impedance estimation.

83.9 ± 4.3% (mean ± SD). The overall R^2 of the parametric model was not significantly different when compared across the four haptic environments ($F_{3,21} = 0.844$; $P = 0.485$). For cross-validated data (50% of data used for fitting; 50% for validation), the average R^2 was 83.1 ± 4.9%. Collectively, these results suggest that the least-squares predictions were robust and not influenced by the environment with which subjects interacted.

The influence of the four tested haptic environments on end-point impedance was characterized by the estimated inertia, viscosity, and stiffness parameters for each subject. The net impedance changes were primarily due to changes in end-point stiffness that were consistent with the characteristics of the haptic environments (Fig. 3). Stiffness ellipsoids estimated during interactions with the environment orthogonal to maximal stiffness were most wide, whereas those estimated during interactions with the high-strength environment aligned to maximal stiffness were elongated and narrower(Fig. 3*D*). The orientation of the estimated end-point stiffness ellipsoids was consistent across environments. The changes observed across all subjects are characterized in detail below.

Adaptation of End-Point Stiffness to Different Haptic Environments

Interactions with destabilizing environments, with a stiffness magnitude greater than that of the arm along the same direction, led to directionally appropriate increases in end-point stiffness. This was determined by quantifying changes in the magnitude of the three principal axes of end-point stiffness (Fig. 4*A*). The magnitude of the primary principal axis of stiffness was influenced significantly by the destabilizing environment ($F_{3,21} = 11.5$; $P < 0.001$) and was greatest during interactions with the high-strength environment aligned with the primary principal axis. Post hoc comparisons revealed that stiffness along the primary principal axis was significantly greater during interactions with the high-strength destabilizing environment than during interactions with the lower-strength environment in the same direction or with the rigid environment. Stiffness along the primary axis was also greater during interactions with the destabilizing environment orthogonal to the direction of maximal stiffness compared with that estimated during interactions with the rigid environment.

The magnitude of the secondary principal axis of end-point stiffness was also adapted to the environment (Fig. 4*A*; $F_{3,21} = 6.97$; $P < 0.002$). It was greatest during interactions with the destabilizing environment oriented along the same direction, referred to as the orthogonal environment. The magnitude of the secondary axis was significantly greater during interactions with the orthogonal environment than during interactions with the rigid environment or with the low-strength environment aligned to the direction of maximal stiffness. The magnitude of the secondary axis was also significantly greater during interactions with the high-strength environment aligned to maximal stiffness than it was during interactions with the rigid environment.

The magnitude of the third principal axis of stiffness was much smaller than the first two principal axes but also varied in magnitude across the tested environments (Fig. 4*A*; $F_{3,21} = 7.1$; $P = 0.002$). It was significantly greater during interactions with the destabilizing environment orthogonal to the direction of maximal stiffness than during interactions with the rigid environment or the low-strength environment, also aligned to maximal stiffness. Stiffness along the third principal axis was also greater during interactions with the high-strength environment aligned to maximal stiffness than during interactions with the rigid environment. Together, these results demonstrate directionally appropriate changes in end-point stiffness, coupled with changes in other directions that are not necessarily solely for stabilizing the haptic environment.

The orientation of the end-point stiffness ellipsoids was largely consistent across environments (Fig. 4*B*). The relative change in stiffness orientation across the environments was not significant for rotations about the first two principal axes (both $F_{3,21} < 1.93$; $P > 0.16$). The environment did have a statistically significant effect for rotations about the third principal axis ($F_{3,21} = 3.36$; $P = 0.04$), although this effect resulted in a rotation of <6° between the most differently oriented environments, for which post hoc comparisons detected a significant difference.

Because the greatest amount of stiffness adaptation occurred along the primary and secondary axes of end-point stiffness, we examined changes in the shape of the estimated stiffness ellipsoids along the plane defined by those axes. The effect of the haptic environment on the calculated shape was significant (Fig. 5*A*; $F_{3,21} = 4.207$; $P = 0.018$). Ellipsoids estimated during interactions with the orthogonal environment were significantly wider than those estimated during interactions with the high-strength and low-strength destabilizing environments aligned to maximal stiffness.

Hogan et al. (1985) suggested that asymmetric reflex feedback could contribute to an antisymmetric component of end-point stiffness. The antisymmetric stiffness, expressed as a percentage of the symmetric stiffness, was influenced significantly by the environment (Fig. 5*B*; $F_{3,21} = 4.751$; $P = 0.011$). This ratio was smaller during interactions with the high-strength destabilizing

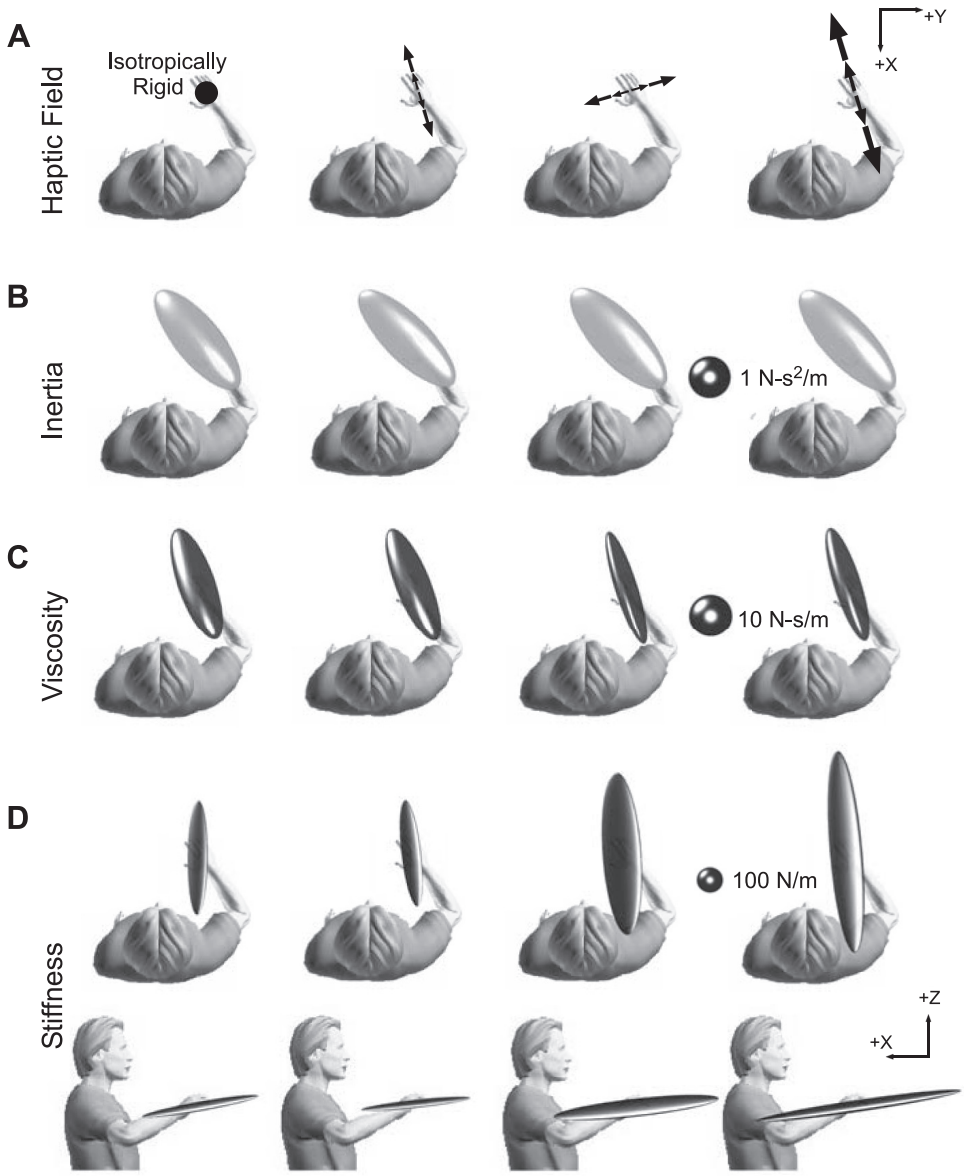

Fig. 3. Representative end-point inertia, viscosity, and stiffness ellipsoids estimated during interactions with all tested environments. All data are from a single subject. *A*: characters depict the tested environments, as seen from above. The black arrows represent the orientation of the unstable haptic environments. Larger arrows are used to denote the high-strength environment; the circle is used to denote the isotropically rigid environment. *B*: end-point inertia ellipsoids; *C*: end-point viscosity ellipsoids; *D*: 2 projections of the estimated end-point stiffness ellipsoid.

environment aligned to maximal stiffness than during interactions with the destabilizing environment orthogonal to maximal stiffness or with the isotropically rigid environment.

There was no noticeable change in the stiffness measured in each environment over the time course of these experiments. This was assessed by computing the stiffness for each subject, using the first and last two perturbations (applied in each of the six perturbation directions) collected at the beginning and end of each experimental condition, and comparing the resulting estimates. The magnitude of each principal axis was compared separately. No significant differences were found among the first ($F_{1,52} = 0.354$; $P = 0.56$), second ($F_{1,52} = 1.513$; $P = 0.224$), or third ($F_{1,52} = 0.328$; $P = 0.57$) principal axes estimated from the data collected at the beginning and end of each experiment.

Adaptation of End-Point Viscosity and Inertia to Different Haptic Environments

There was no statistically significant change in end-point viscosity during interactions with the tested haptic environments. This was true for both magnitude (all $F_{3,21} < 3.066$; all $P > 0.050$) and orientation (all $F_{3,21} < 2.0$; all $P > 0.15$). This lack of statistical significance, however, may be attributable, at least in part, to the variability of the estimated end-point viscosities, as reported previously (Perreault et al. 2004).

The magnitude of the estimated end-point inertia was also invariant across environments, as would be expected (all $F_{3,21} < 1.437$; all $P > 0.260$). However, there was a small but significant change in the orientation of end-point inertia relative to the second primary axis ($F_{3,21} = 3.86$; $P = 0.02$). Post hoc comparisons indicated that this resulted from a significant rotation when subjects interacted with the orthogonal environment relative to that measured during interactions with the stiff environment. This change in orientation was small ($\Delta = 5.0°$). The results were similar for rotations about the first and third principal axes of end-point inertia, although these rotations did not reach statistical significance (both $F_{3,21} < 2.7$; both $P > 0.07$). Since the mass of the limb was constant across all experiments for each subject, this change was likely dominated by a small but consistent change in

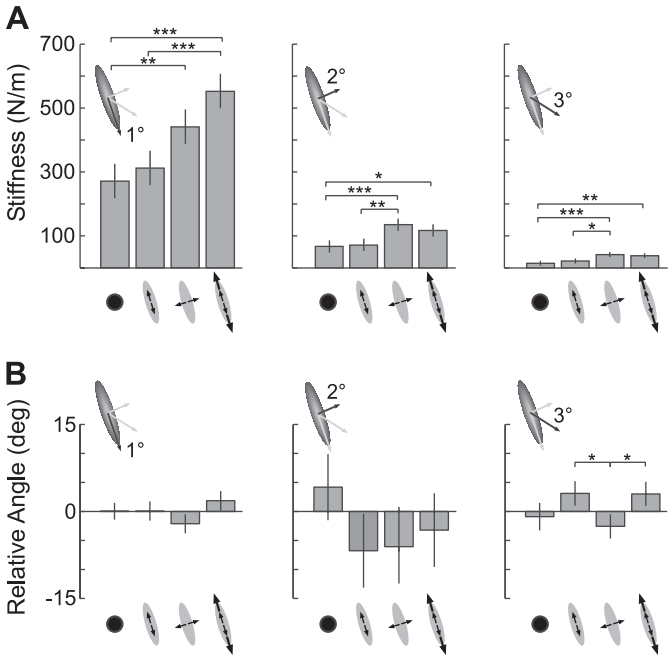

Fig. 4. Influence of environment on the estimated end-point stiffness. *A*: end-point stiffness magnitude for each environment; results are shown separately for each principal axis. *B*: rotation of each principal axis relative to the average orientation recorded across all subjects and environments. Rotations were computed in the following order: primary axis, secondary axis, tertiary axis. Notation for environments is as shown in Fig. 3*A*. Bars are means ± SE. Statistically significant comparisons among environments are indicated by: $*P < 0.05$, $**P < 0.01$, and $***P < 0.001$.

arm posture across the different environments. A post hoc analysis of the wrist position, as measured by the optical tracking system, indicated a change of 5.2 mm ($P < 0.001$) between the rigid and orthogonal environments, corresponding to an average forearm rotation of ~4° across subjects.

There were no changes in the magnitude of the viscosity or inertial ellipsoids during the course of these experiments. This was assessed by comparing the principal axes for these parameter ellipsoids when estimated from data collected at the beginning and end of each experimental condition, as described above for the end-point stiffness. No significant difference was noted for any principal axis of either parameter ellipsoid (all $P > 0.38$).

DISCUSSION

This study examined how the end-point impedance of the human arm is adapted during postural tasks that compromise arm stability. Specifically, we considered 3D negative-stiffness environments that compromise arm stability along a specific direction. Our results demonstrated that arm impedance is modulated to compensate for environmental instabilities during postural tasks. These changes were primarily in the magnitude of end-point stiffness, the static component of impedance, which was found to increase in the direction of the environmental instability. There were no significant changes in the orientation of maximal stiffness during interactions with the tested environments. Furthermore, there were no significant changes in the magnitude of end-point viscosity or inertia, suggesting that the primary change to arm impedance was a selective increase in stiffness to compensate for the destabilizing stiffness properties of the environment. We suggest that at a fixed posture, interactions with preferentially unstable environments drive moderate, task-appropriate changes in limb mechanics that are tuned to the environment. However, more task-appropriate and more drastic shifts in end-point stiffness could be made if the arm were unconstrained, and posture could be shifted.

Influence of Environment Instability on End-Point Impedance

During interactions with directionally destabilizing environments, there was a preferential increase in the size and shape of end-point stiffness along the direction of the instability. End-point stiffness magnitude was increased during interactions with destabilizing environments, where the magnitude of negative stiffness exceeded—or in some cases, approached—that of the maximal measured arm stiffness, along the direction of the environment. These results suggest that limb mechanics are adapted to compensate for interactions with environments that compromise limb stability. This finding is consistent with earlier studies involving a 2D workspace (Rancourt and Hogan 2001; Selen et al. 2009). The present results demonstrated task-appropriate, albeit modest, changes in 3D end-point stiffness that were tuned, not only to the directional properties of the negative-stiffness environments but also to their strength.

End-point stiffness increased in the direction of the destabilizing environment, but the observed changes in stiffness were not restricted to that direction. For example, stiffness along the primary axis increased significantly (relative to that measured during interactions with the rigid environment), even when the unstable haptic environment was oriented along the direction of the secondary end-point stiffness axis (Fig. 4*A*). Hence, whereas the change in stiffness for each axis was always greatest when interacting with an unstable environment oriented along that same direction, those changes were not observed in isolation. This is not surprising, given that muscle stiffness is not generally aligned with the primary axes of end-point stiffness, but it does highlight the importance of considering limb biomechanics when assessing the flexibility of the nervous system in controlling end-point mechanics (Flash and Mussa-Ivaldi 1990; Hu et al. 2011).

The observed changes in stiffness geometry during our postural studies were dramatically more modest than those observed previously during movement (Burdet et al. 2001;

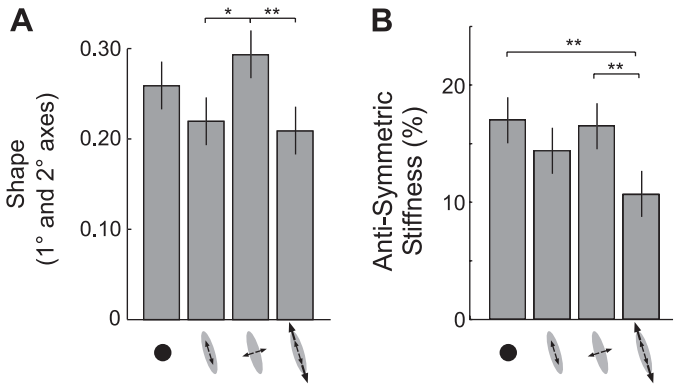

Fig. 5. Influence of environment on the shape (*A*) and antisymmetric components (*B*) of end-point stiffness. Notation for environments is as shown in Fig. 3*A*. Bars are means ± SE. Statistically significant comparisons between environments are indicated by: $*P < 0.05$ and $**P < 0.01$.

Franklin et al. 2007; Kadiallah et al. 2011). Specifically, the observed changes in stiffness magnitude were not sufficient to substantially change stiffness orientation during the postural tasks. This limited ability to reorient the direction of maximal stiffness has been reported in previous postural studies (Darainy et al. 2004; Perreault et al. 2002; Selen et al. 2009), but none of the previous works matched the unstable environments commonly used in the movement studies. Our present results demonstrate that the inability to reorient end-point stiffness cannot be attributed to the properties of the haptic environment but rather, represent a fundamental difference between the control of arm mechanics during posture and movement (Darainy et al. 2007; Lametti et al. 2007). They may also reflect the fact that during postural tasks, a reorientation of end-point stiffness is often not the most efficient means to increase stiffness in a specific direction (Hu et al. 2012).

The observed changes in end-point impedance were largely restricted to stiffness. There were no significant changes in the magnitude or orientation of end-point viscosity. This finding likely reflects a specificity to the haptic environments used in these experiments, rather than an inability to control end-point viscosity (Lacquaniti et al. 1993). There were also no observed changes in the magnitude of end-point inertia, as would be expected during the course of a single experiment. We did observe minor changes in the orientation of end-point inertia during interactions with the different environments. These changes were within the tolerance of the postural feedback provided to the subject and likely represent small but consistent changes in arm posture during these experiments. Even though our paradigm allowed for only minor changes in arm posture, this finding is consistent with previous studies demonstrating that subjects choose postures that optimize end-point stiffness for the task at hand (Trumbower et al. 2009).

Subjects were able to adapt end-point stiffness rapidly, as evidenced by the lack of a learning effect during the time course of our experiments. Our inability to observe the time course of stiffness adaptation is not surprising, given the nature of our experiments, which were not explicitly designed to study this feature. Our protocol used perturbations in six different directions. Prior to each perturbation, the subject interacted with the unstable field for a minimum of ~1 s. Often, subjects were in the target for longer periods of time, allowing ample opportunity to interact with and learn the unstable field. Even when making rapid movements (~600 ms) in similar fields, subjects adapt within 10–20 trials (Franklin et al. 2003). Hence, our experiments simply may not have had the time resolution required to observe the time course of learning required for our experimental task. Rather, it appears that subjects had adapted completely by the time that the first stiffness measurement in each environment was complete.

Mechanisms of Stiffness Control

A number of mechanisms may have contributed to the observed changes in end-point stiffness. Changes in co-contraction can be adapted rapidly by a subject (Franklin et al. 2003) and generalized (Gribble et al. 2003), or preferential (Gribble and Ostry 1998) changes in co-contraction may have been used by our participants. In experimental conditions similar to those tested here (Krutky et al. 2010), we recorded an increase in the amount of co-contraction used during interactions with environments orthogonal to maximal stiffness relative to that during interactions with the other tested environments. These changes, however, were small (<1% maximal voluntary contraction) and are unlikely to account for the nearly twofold changes in stiffness reported in this study. This previous work also demonstrated substantial changes in stretch reflexes elicited by perturbations similar to those in the present study. For perturbations in the plane of the instabilities used in the present study, our reflex activity reported previously (measured using electromyography) was 50–100% greater than the background muscle activity measured prior to the perturbation. Hence, those results suggest that reflexes could have contributed substantially to the changes in stiffness reported here. This would be consistent with work suggesting that reflex responses can contribute to preferential changes in end-point stiffness reported during reaching movements (Franklin et al. 2007). Interestingly, the work by Franklin and coauthors (2007) suggested that reflex adaptation may contribute to stiffness modulation based on the finding that stiffness asymmetry increased during interactions with specific environments (Hogan 1985). We found significant differences in stiffness asymmetry during interactions with the two haptic environments that most compromised arm stability and induced the greatest amount of stiffness adaptation (Fig. 5). Reflex contributions to stiffness adaptation during interactions with unstable environments would also be consistent with their reported role in stiffness modulation during interactions with compliant environments (Doemges and Rack 1992a; Mugge et al. 2010) and with anticipatory changes in reflex gain reported previously (Kimura et al. 2006; Lacquaniti and Maioli 1989).

Finally, rapid voluntary or triggered responses may also have contributed to the observed results. Our methods for estimating impedance included data up to 210 ms, following perturbation onset. Therefore, any muscle activity that could have generated force responses within 210 ms of perturbation onset may have contributed to our findings. For this reason, it is impossible to rule out contributions from rapid voluntary responses or triggered reactions to the applied perturbations. The latter can initiate muscle activity as early as ~70 ms following perturbation onset (Crago et al. 1976; Lewis et al. 2006). Regardless of the mechanism, our results clearly demonstrate that the nervous system can adapt the involuntary response to postural perturbations in a manner that provides rapid compensation during interactions with unstable environments.

The mechanisms contributing to the differences in stiffness modulation observed during posture and movement are less clear. There is evidence that different cortical mechanisms are involved in the control of posture and movement (Kurtzer et al. 2005), and these differences could contribute to different feedback responses for reflexes that pass through the cortex (Kimura et al. 2006; Pruszynski et al. 2011; Shemmell et al. 2009). The transient nature of the muscle activations during movement tasks may also be important, allowing for corrective actions that might destabilize the limb during maintained posture (Bunderson et al. 2008; Selen et al. 2009). Finally, joint stiffness can decrease dramatically during dynamic conditions (Bennett et al. 1992; MacNeil et al. 1992), potentially allowing the type of modulation reported in the current work to have a larger net influence on the impedance of the arm. Thus movement through destabilizing environments, rather than simply interacting with these environments, may be necessary to drive

the reorientation of maximal end-point stiffness toward the direction of the instability.

Functional Implications

Whereas our study focused on responses to externally imposed perturbations of posture, it is interesting to consider how our results relate to the maintenance of posture during unperturbed conditions, such as holding a weight above the head or standing quietly. Stiffness regulation is only one approach to maintaining stability during such functionally relevant tasks. For the lower limb, it has been suggested that stiffness regulation alone is not sufficient to maintain balance (Loram and Lakie 2002; Morasso 1981) and that it works in concert with slower feedback mechanisms to achieve stability (Finley et al. 2012). Feedback control has also been implicated in the control of unperturbed arm posture when interacting with unstable loads (Lakie et al. 2003), and it is likely to have contributed to the subjects' ability to remain in the postural targets prior to the perturbations used in this study. This possibility is supported by the observations of how end-point tracking accuracy prior to the perturbation depended on the characteristics of the haptic environment, with less stable environments leading to larger tracking errors. Such dependence implies that feedback contributes to stabilization. Our previous work has shown that long-latency stretch reflexes are at least part of this feedback response, although their contributions do not preclude the use of longer latency pathways commonly associated with volitional control, and are less likely to have contributed to our experimental estimates of stiffness.

Estimates of stiffness depend strongly on the characteristics of the perturbations used in the estimation process, with smaller and faster perturbations leading to larger stiffness estimates (Kirsch et al. 1994; Rack and Westbury 1974). This relationship can be seen by comparing the estimates from the preliminary experiments using small, stochastic perturbations with the primary experiments using larger ramp perturbations. The relevance of these different estimates to functional tasks depends on the magnitude of the perturbations encountered during the task. For example, the magnitude of the postural deviations in the absence of perturbations ranged from 2 mm to 4 mm in the present study, a value similar to the SD of the stochastic perturbation used in the preliminary experiment. Hence, the estimates of stiffness from the preliminary experiment are likely to be most relevant to tasks with small motions, such as unperturbed posture, whereas those obtained using the larger ramp perturbations of the primary experiment are likely most relevant to tasks in which larger external perturbations are encountered. In contrast to stiffness magnitude, orientation is not sensitive to perturbation size (Krutky 2009), suggesting that our main conclusions regarding the ability to modulate stiffness orientation are robust across postural tasks involving a broad range of perturbation types.

Our data suggest that at a fixed posture, the degree to which end-point stiffness orientation can be adapted to the functional requirements of a task is limited. Changes in posture have, however, been shown to have a profound effect on the orientation of maximal arm stiffness (Flash and Mussa-Ivaldi 1990; Mussa-Ivaldi et al. 1985). Furthermore, during unconstrained tasks, posture selection is readily used to adapt end-point stiffness to the stability requirements of a task (Trumbower et al. 2009). Together, these findings suggest that the stiffness adaptation quantified here represents an involuntary, early reaction to stabilize the arm before more effective corrections, such as a change in posture or voluntary forces, can be enacted.

ACKNOWLEDGMENTS

The authors thank Timothy Haswell and Vengateswaran Ravichandran for their technical assistance and Eileen Krepkovich for her skillful editing. The authors are also grateful to all study participants.

GRANTS

Support for this work was provided by American Heart Association Predoctoral Fellowship 0615573Z and National Institute of Neurological Disorders and Stroke Grant R01 NS053813.

DISCLOSURES

No conflicts of interest, financial or otherwise, are declared by the authors.

AUTHOR CONTRIBUTIONS

Author contributions: M.A.K. and E.J.P. conception and design of research; M.A.K. and R.D.T. performed experiments; M.A.K., R.D.T., and E.J.P. analyzed data; M.A.K., R.D.T., and E.J.P. interpreted results of experiments; M.A.K. and R.D.T. prepared figures; M.A.K. and R.D.T. drafted manuscript; M.A.K., R.D.T., and E.J.P. edited and revised manuscript; M.A.K., R.D.T., and E.J.P. approved final version of manuscript.

REFERENCES

Akazawa K, Milner TE, Stein RB. Modulation of reflex EMG and stiffness in response to stretch of human finger muscle. *J Neurophysiol* 49: 16–27, 1983.

Bennett DJ, Hollerbach JM, Xu Y, Hunter IW. Time-varying stiffness of the human elbow joint during cyclic voluntary movement. *Exp Brain Res* 88: 433–442, 1992.

Bunderson NE, Burkholder TJ, Ting LH. Reduction of neuromuscular redundancy for postural force generation using an intrinsic stability criterion. *J Biomech* 41: 1537–1544, 2008.

Burdet E, Osu R, Franklin DW, Milner TE, Kawato M. The central nervous system stabilizes unstable dynamics by learning optimal impedance. *Nature* 414: 446–449, 2001.

Crago PE, Houk JC, Hasan Z. Regulatory actions of human stretch reflex. *J Neurophysiol* 39: 925–935, 1976.

Darainy M, Malfait N, Gribble PL, Towhidkhah F, Ostry DJ. Learning to control arm stiffness under static conditions. *J Neurophysiol* 92: 3344–3350, 2004.

Darainy M, Towhidkhah F, Ostry DJ. Control of hand impedance under static conditions and during reaching movement. *J Neurophysiol* 97: 2676–2685, 2007.

Dietz V, Discher M, Trippel M. Task-dependent modulation of short- and long-latency electromyographic responses in upper limb muscles. *Electroencephalogr Clin Neurophysiol* 93: 49–56, 1994.

Doemges F, Rack PM. Changes in the stretch reflex of the human first dorsal interosseous muscle during different tasks. *J Physiol* 447: 563–573, 1992a.

Doemges F, Rack PM. Task-dependent changes in the response of human wrist joints to mechanical disturbance. *J Physiol* 447: 575–585, 1992b.

Finley JM, Dhaher YY, Perreault EJ. Contributions of feed-forward and feedback strategies at the human ankle during control of unstable loads. *Exp Brain Res* 217: 53–66, 2012.

Flash T, Mussa-Ivaldi FA. Human arm stiffness characteristics during the maintenance of posture. *Exp Brain Res* 82: 315–326, 1990.

Franklin DW, Liaw G, Milner TE, Osu R, Burdet E, Kawato M. Endpoint stiffness of the arm is directionally tuned to instability in the environment. *J Neurosci* 27: 7705–7716, 2007.

Franklin DW, Osu R, Burdet E, Kawato M, Milner TE. Adaptation to stable and unstable dynamics achieved by combined impedance control and inverse dynamics model. *J Neurophysiol* 90: 3270–3282, 2003.

Franklin DW, So U, Kawato M, Milner TE. Impedance control balances stability with metabolically costly muscle activation. *J Neurophysiol* 92: 3097–3105, 2004.

Gomi H, Osu R. Task-dependent viscoelasticity of human multijoint arm and its spatial characteristics for interaction with environments. *J Neurosci* 18: 8965–8978, 1998.

Gribble PL, Mullin LI, Cothros N, Mattar A. Role of cocontraction in arm movement accuracy. *J Neurophysiol* 89: 2396–2405, 2003.

Gribble PL, Ostry DJ. Independent coactivation of shoulder and elbow muscles. *Exp Brain Res* 123: 355–360, 1998.

Hogan N. The mechanics of multi-joint posture and movement control. *Biol Cybern* 52: 315–331, 1985.

Hu X, Murray WM, Perreault EJ. Biomechanical constraints on the feedforward regulation of endpoint stiffness. *J Neurophysiol* 108: 2083–2091, 2012.

Hu X, Murray WM, Perreault EJ. Muscle short-range stiffness can be used to estimate the endpoint stiffness of the human arm. *J Neurophysiol* 105: 1633–1641, 2011.

Kadiallah A, Liaw G, Kawato M, Franklin DW, Burdet E. Impedance control is selectively tuned to multiple directions of movement. *J Neurophysiol* 106: 2737–2748, 2011.

Kearney RE, Stein RB, Parameswaran L. Identification of intrinsic and reflex contributions to human ankle stiffness dynamics. *IEEE Trans Biomed Eng* 44: 493–504, 1997.

Kimura T, Haggard P, Gomi H. Transcranial magnetic stimulation over sensorimotor cortex disrupts anticipatory reflex gain modulation for skilled action. *J Neurosci* 26: 9272–9281, 2006.

Kirsch RF, Boskov D, Rymer WZ. Muscle stiffness during transient and continuous movements of cat muscle: perturbation characteristics and physiological relevance. *IEEE Trans Biomed Eng* 41: 758–770, 1994.

Krutky MA. *Neural and Mechanical Contributions to the Regulation of Human Arm Impedance in Three Degrees of Freedom* (PhD thesis). Evanston, IL: Dept. of Biomedical Engineering, Northwestern Univ., 2009.

Krutky MA, Ravichandran VJ, Trumbower RD, Perreault EJ. Interactions between limb and environmental mechanics influence stretch reflex sensitivity in the human arm. *J Neurophysiol* 103: 429–440, 2010.

Krutky MA, Trumbower RD, Perreault EJ. Effects of environmental instabilities on endpoint stiffness during the maintenance of human arm posture. *Conf Proc IEEE Eng Med Biol Soc* 2009: 5938–5941, 2009.

Kurtzer I, Herter TM, Scott SH. Random change in cortical load representation suggests distinct control of posture and movement. *Nat Neurosci* 8: 498–504, 2005.

Lacquaniti F, Carrozzo M, Borghese NA. Time-varying mechanical behavior of multijointed arm in man. *J Neurophysiol* 69: 1443–1463, 1993.

Lacquaniti F, Maioli C. The role of preparation in tuning anticipatory and reflex responses during catching. *J Neurosci* 9: 134–148, 1989.

Lakie M, Caplan N, Loram ID. Human balancing of an inverted pendulum with a compliant linkage: neural control by anticipatory intermittent bias. *J Physiol* 551: 357–370, 2003.

Lametti DR, Houle G, Ostry DJ. Control of movement variability and the regulation of limb impedance. *J Neurophysiol* 98: 3516–3524, 2007.

Lewis GN, MacKinnon CD, Perreault EJ. The effect of task instruction on the excitability of spinal and supraspinal reflex pathways projecting to the biceps muscle. *Exp Brain Res* 174: 413–425, 2006.

Lewis GN, Perreault EJ, Mackinnon CD. The influence of perturbation duration and velocity on the long-latency response to stretch in the biceps muscle. *Exp Brain Res* 163: 361–369, 2005.

Ljung L. *System Identification Theory for the User*. Upper Saddle River, NJ: Prentice-Hall, 1999.

Loram ID, Lakie M. Human balancing of an inverted pendulum: position control by small, ballistic-like, throw and catch movements. *J Physiol* 540: 1111–1124, 2002.

MacNeil JB, Kearney RE, Hunter IW. Identification of time-varying biological systems from ensemble data. *IEEE Trans Biomed Eng* 39: 1213–1225, 1992.

Matthews PB. Observations on the automatic compensation of reflex gain on varying the pre-existing level of motor discharge in man. *J Physiol* 374: 73–90, 1986.

McIntyre J, Mussa-Ivaldi FA, Bizzi E. The control of stable arm postures in the multi-joint arm. *Exp Brain Res* 110: 248–264, 1996.

Morasso P. Spatial control of arm movements. *Exp Brain Res* 42: 223–227, 1981.

Mugge W, Abbink DA, Schouten AC, Dewald JP, van der Helm FC. A rigorous model of reflex function indicates that position and force feedback are flexibly tuned to position and force tasks. *Exp Brain Res* 200: 325–340, 2010.

Mussa-Ivaldi FA, Hogan N, Bizzi E. Neural, mechanical, and geometric factors subserving arm posture in humans. *J Neurosci* 5: 2732–2743, 1985.

Perreault EJ, Chen K, Trumbower RD, Lewis G. Interactions with compliant loads alter stretch reflex gains but not intermuscular coordination. *J Neurophysiol* 99: 2101–2113, 2008.

Perreault EJ, Kirsch RF, Acosta AM. Multiple-input, multiple-output system identification for characterization of limb stiffness dynamics. *Biol Cybern* 80: 327–337, 1999.

Perreault EJ, Kirsch RF, Crago PE. Effects of voluntary force generation on the elastic components of endpoint stiffness. *Exp Brain Res* 141: 312–323, 2001.

Perreault EJ, Kirsch RF, Crago PE. Multijoint dynamics and postural stability of the human arm. *Exp Brain Res* 157: 507–517, 2004.

Perreault EJ, Kirsch RF, Crago PE. Voluntary control of static endpoint stiffness during force regulation tasks. *J Neurophysiol* 87: 2808–2816, 2002.

Pfeifer S, Vallery H, Hardegger M, Riener R, Perreault EJ. Model-based estimation of knee stiffness. *IEEE Trans Biomed Eng* 59: 2604–2612, 2012.

Pruszynski JA, Kurtzer I, Nashed JY, Omrani M, Brouwer B, Scott SH. Primary motor cortex underlies multi-joint integration for fast feedback control. *Nature* 478: 387–390, 2011.

Rack PMH, Westbury DR. The short range stiffness of active mammalian muscle and its effect on mechanical properties. *J Physiol* 240: 331–350, 1974.

Rancourt D, Hogan N. Stability in force-production tasks. *J Mot Behav* 33: 193–204, 2001.

Rohmert W. Ermittung von Erholung-spausen fur statische arbeit des menschen. *Int Angew Physiol* 18: 123–164, 1960.

Selen LP, Franklin DW, Wolpert DM. Impedance control reduces instability that arises from motor noise. *J Neurosci* 29: 12606–12616, 2009.

Shadmehr R, Mussa-Ivaldi FA, Bizzi E. Postural force fields of the human arm and their role in generating multijoint movements. *J Neurosci* 13: 45–62, 1993.

Shemmell J, An JH, Perreault EJ. The differential role of motor cortex in stretch reflex modulation induced by changes in environmental mechanics and verbal instruction. *J Neurosci* 29: 13255–13263, 2009.

Sinkjaer T, Toft E, Andreassen S, Hornemann BC. Muscle stiffness in human ankle dorsiflexors: intrinsic and reflex components. *J Neurophysiol* 60: 1110–1121, 1988.

Trumbower RD, Krutky MA, Yang BS, Perreault EJ. Use of self-selected postures to regulate multi-joint stiffness during unconstrained tasks. *PLoS One* 4: e5411, 2009.

Van der Linde RQ, Lammertse P, Frederiksen E, Ruiter B. The HapticMaster, a new high-performance haptic interface. In: *Proceedings Europtics*. Edinburgh, UK: 2002, p. 1–5.

Westwick DT, Perreault EJ. Closed-loop identification: application to the estimation of limb impedance in a compliant environment. *IEEE Trans Biomed Eng* 58: 521–530, 2011.

Zhang LQ, Rymer WZ. Simultaneous and nonlinear identification of mechanical and reflex properties of human elbow joint muscles. *IEEE Trans Biomed Eng* 44: 1192–1209, 1997.